A.A. Landman and D. de Waal,
*S. Afr. J. Chem.*, 2005, **58**, 46–52,
<http://journals.sabinet.co.za/sajchem/>.



# Modelling Sulphur Clusters for an Understanding of Ultramarine

**Andreas A. Landman and Danita de Waal***

*Department of Chemistry, University of Pretoria, Pretoria 0002, South Africa.*

Received 1 December 2003; revised 9 June 2004; accepted 19 August 2004

ABSTRACT

**Ultramarine pigments are aluminosilicate-based and contain sulphur-based chromophores. Self-consistent-field Hartree-Fock and Møller-Plesset second order perturbation theory were applied to determine the relative stability of $S_2$, $S_2^{-\bullet}$, $S_2^{2-}$, and $S_3$, $S_3^{-\bullet}$, $S_3^{2-}$. The singly charged species was found to be the most stable in both sets. The transition from green to blue ultramarine is thought to be the transformation of the doubly charged species to the singly charged species and is known to be exothermic. Modelling studies supported this hypothesis. The open, $C_{2v}$, isomer was found to be the most stable for the $S_3^{-\bullet}$ molecule, which is the blue chromophore in ultramarine. The closed, $D_{3h}$, geometry represents a transition state. The $S_4$ molecule is the most likely chromophore in ultramarine red; however the specific isomer is uncertain. Under the assumption that $S_4$ was formed by a concerted reaction between $S_3^{-\bullet}$ and $S^{+\bullet}$, a Woodward-Hoffmann analysis of the molecular orbitals of $S_3^{-\bullet}$ and $S^{+\bullet}$ supported the formation of the puckered square $S_4$, pyramidal $S_4$, double triangle $S_4$, and gauche $S_4$ chain isomers. The gauche $S_4$ chain is the most likely isomer in ultramarine red.**

KEYWORDS

**Ultramarine pigments, Woodward-Hoffmann analysis, modelling.**

## 1. Introduction

Ultramarine pigments come in green, blue, greenish blue, reddish blue, violet, pink and red variants.[1–7] Several chromophores are present in the aluminosilicate zeolite-type framework of the ultramarine species. $S_2^{-\bullet}$ is the yellow chromophore[2,5,8–10] in ultramarine and $S_3^{-\bullet}$ (Fig. 1) is the blue chromophore.[2,5,8,9] Ultramarine green is an ultramarine species in which the yellow and blue chromophores are present in such a ratio as to allow the green colour to be observed.

Ultramarine blue is synthesized in two steps, a reduction step followed by an oxidation step.[1,2,5,8,9,11–16] The nature of these steps is, however, disputed. Some authors suggested Equation 1,[2,5,8,9] whereas others supported the existence of doubly charged species according to Equations 2 and 3.[1,11–15]

$$\underset{\text{Yellow}}{S_8} \xrightarrow{\text{Reduction}} \underset{\text{Yellow}}{S_2^{-\bullet}} \xrightarrow{\text{Oxidation}} \underset{\text{Blue}}{S_3^{-\bullet}} \quad (1)$$

$$2Na_8[Al_6Si_6O_{24}]S_{2-3} + SO_2 + O_2 \rightarrow 2Na_7[Al_6Si_6O_{24}]S_{2-3} + Na_2SO_4 \quad (2)$$

$$2\,S_{2-3}^{2-}(s) + SO_2(g) + O_2(g) \rightarrow 2\,S_{2-3}^{-}(s) + 2\,S_4^{2-} \quad (3)$$

The oxidation of ultramarine green to ultramarine blue is related to an increasing $S_3^{-\bullet}/S_2^{-\bullet}$ ratio,[2,5,8,9,16] in support of Equation 1. Beardsley and Whiting[12] described the formation of ultramarine blue with oxygen as oxidizing agent and introduced the use of $SO_2$ in the production thereof.[12] Gorshtein[11,14] successfully explained the formation of $Na_2SO_4$ and the role of $SO_2$ (Equations 2 and 3), noted by Tarling and co-workers[17] and Gobeltz and co-workers.[8] This explanation was based on the identification of $S_3^{2-}$ *and* $S_2^{2-}$ as the yellow, and $S_3^{-\bullet}$ *and* $S_2^{-\bullet}$ as the blue chromophores. Other evidence identified $S_3^{-\bullet}$ as responsible for the blue and $S_2^{-\bullet}$ for the yellow colour.[2,5,8,9,18] No spectroscopic evidence of the doubly charged species is available in the literature.[16] Köhler and co-workers[10] synthesized ultramarine yellow from the thiocyanide derivative of sodalite. They confirmed that the yellow chromophore was $S_2^{-\bullet}$ and that oxidation led to the formation of ultramarine green, with the simultaneous formation of $S_3^{-\bullet}$.[10] The evidence supported the formation of $S_3^{-\bullet}$ from $S_2^{-\bullet}$ rather than from $S_3^{2-}$.

Weller and co-workers,[19] who also synthesized ultramarine from thiocyanate sodalites, concluded that a colourless polysulphide sodalite was the initial product at high temperatures. This initial product was assumed to undergo a secondary in-cage reaction to produce the coloured polysulphide radical anions *in situ* by heating in $SO_2$ at about 500°C.[19] The presence of a doubly-charged species was inferred from the formation of a noselite-like (nosean) phase.[19] The high ratio of sulphur atoms to unpaired electrons found by Hofmann and co-workers[6] in the ultramarine green pigment supported the possible existence of doubly-charged, non-radical sulphide species. This conclusion was not generally accepted.[20]

The ultramarine red chromophore had been identified as the $S_4$ molecule (Fig. 2).[1,2,5,21] In order to identify the $S_4$ isomer it was assumed that $S_4$ was formed from $S_3^{-\bullet}$ and $S^{+\bullet}$ in a concerted reaction.[22] The feasibility of single-step concerted reaction products could be evaluated by examining the phase symmetry of the molecular orbitals, by the methods of Fukui[23,24] and of Woodward and Hoffmann.[25–27] The highest occupied molecular orbital (HOMO) and lowest unoccupied molecular orbital

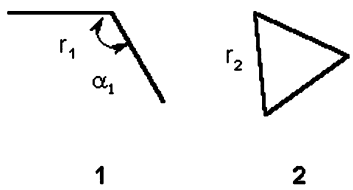


**Figure 1**. $S_3$ isomers: (1) open ($C_{2v}$), (2) closed ($D_{3h}$)

*To whom correspondence should be addressed.
E-mail address: danita.dewaal@up.ac.za

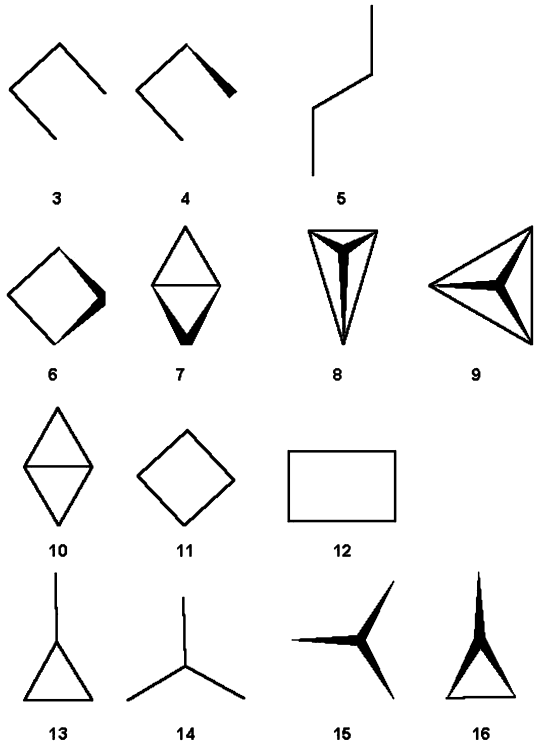


**Figure 2**. Possible $S_4$ isomers: (**3**) *cis* chain ($C_{2v}$), (**4**) gauche chain ($C_2$), (**5**) *trans* chain ($C_{2h}$), (**6**) puckered ring ($D_{2d}$), (**7**) butterfly ($D_{2d}$), (**8**) tetrahedral (geometry optimized) ($D_{2d}$), (**9**) tetrahedral ($T_d$), (**10**) double triangle ($D_{4h}$), (**11**) square planar ($D_{4h}$), (**12**) rectangle ($D_{2h}$), (**13**) exocyclic ($C_{2v}$), (**14**) branched chain ($D_{3h}$), (**15**) pyramidal ($C_s$), (**16**) bent exocyclic ($C_s$)

(LUMO) were assumed to feature in reactions to form new bonds. For a reaction to take place the HOMO (LUMO) of the attacked species and the LUMO (HOMO) of the attacking species need to have the same phase symmetry. This condition allowed regions of the same phase in the molecular orbitals to overlap and to form new bonding and antibonding molecular orbitals provided favourable overlap occurred.

In this study the different possible $S_4$ isomers were evaluated in a modified Woodward-Hoffmann symmetry correlation analysis, similar to that applied by Carey and Sundberg.[28] The current method modelled the molecular orbitals of the reactants, without modelling the molecular orbitals of the $S_4$ products. Sannigrahi and Grein[29] used the Woodward-Hoffmann methodology to show that the formation of $S_4^{2+}$ from $S_2^{+}$ was not allowed.

The molecular orbitals of $S^{+\bullet}$, $S_2^{-\bullet}$ and $S_3^{-\bullet}$ were computed in this work in order to use a Woodward-Hoffmann analysis to evaluate the feasibility of the formation of the possible $S_4$ isomers. $S_2$, $S_2^{2-}$, $S_3$ and $S_3^{2-}$ were also modelled in an effort to find the most stable sulphur species. These results might confirm that green ultramarine yielded blue ultramarine by the formation of $S_2^{-\bullet}$, $S_3^{-\bullet}$ from $S_2^{2-}$, $S_3^{2-}$.[11–15]

## 2. Experimental Data

Naudé[30,31] studied the rotational spectrum of $S_2$ and determined the bond length to be 1.893 Å. Based on the absorption band fine structure between 160 and 190 nm, Maeder and Miescher[32] calculated a vibrational wavenumber of 724 cm$^{-1}$ for $S_2$. $S_2^{-\bullet}$ had a Raman band at 590 cm$^{-1}$,[2,5] and $S_2^{2-}$ a band at 451 cm$^{-1}$.[33]

Hopkins and co-workers[34] observed the $S_3$ molecule as part of an electric discharge reaction and observed Raman bands at 490, 585 and 650 cm$^{-1}$. Brabson and co-workers[35] recorded the infrared spectrum of $S_3$ in a solid argon matrix (Table 1). They concluded that the structure of $S_3$ was the $C_{2v}$ open geometry, with a bond angle of 116 ± 2°.[35] Lenain and co-workers[36] studied the Raman spectrum of $S_3$ and also concluded that the observed species was the $C_{2v}$ isomer (Table 1). Clark and Cobbold[2] observed both the Raman and infrared bands for $S_3^{-\bullet}$ (Table 1). Janz and co-workers[33,37,38] studied several polysulphides. For $BaS_3$ the $S_3^{2-}$ structure was said to be $C_{2v}$ with vibrational bands at 227/238 (R), 458 (R,IR) and 476 cm$^{-1}$ (R,IR).[37] For $K_2S_3$ the same interpretation held, with the stretching modes accidentally degenerate: 238 (R) and 466 cm$^{-1}$ (R,IR).[38]

**Table 1**. Experimental characteristics of $S_3$, $S_3^{-\bullet}$ and $S_3^{2-}$ species.

| Species | Assignment | Wavenumber/cm$^{-1}$ | | Reference |
|---|---|---|---|---|
| | | Infrared | Raman | |
| $S_3$ | $\nu_1$ | | 585 | [34] |
| | $\nu_2$ ? | 495 or 310 | 490 | |
| | $\nu_3$ | | 650 | |
| | $\nu_1$ | | 583 | [35] |
| | $\nu_2$ | 680 | | [35,37] |
| | Vibrational progression | 340<br>450 | | [35,39] |
| | $\nu_1$ | | 575 | [36] |
| | $\nu_2$ | | 256 | |
| | $\nu_3$ | | 656 | |
| $S_3^{-\bullet}$ | $\nu_1$ | | 548 | [2,5] |
| | $\nu_3$ | 582 | | [2] |
| | $\nu_1$ | 547 | | [2] |
| | $\nu_2$ | | 232 | [40] |
| $S_3^{2-}$ | $\nu_1$ or $\nu_3$ | 457 | 458 | [37] |
| | $\nu_2$ | | 227/238 | |
| | $\nu_1$ or $\nu_3$ | 476 | 476 | |
| | $\nu_1$ and $\nu_3$ | | 466 | [38] |
| | $\nu_2$ | | 238 | |

## 3. Molecular Modelling

HyperChem[41] was used to perform the computations on a Compaq Pressario 1200 Celeron 850 MHz processor with 128 MB RAM.

In the work on sulphur compounds the shapes of the molecular orbitals were important because they dictated the reactivity of the species under consideration and were used in the Woodward-Hoffmann analyses. The energies were also important as an estimate of the relative stability of the ionic states of $S_2$ and $S_3$. A potential energy surface specified the classical potential energy as a function of molecular structure.[42] This concept was useful for the comparison of the possible geometrical isomers. The potential energy surface was inspected for $S_2$, $S_2^{-\bullet}$, $S_2^{2-}$, $S_3$, $S_3^{-\bullet}$ and $S_3^{2-}$ in an effort to find the most favourable oxidation states of these species, and to obtain the molecular orbitals for use in a Woodward-Hoffmann analysis.

A disadvantage inherent in all the computations was that the data obtained were related to gas phase molecules in vacuum at 0 K. No interaction between molecules within a crystal was taken into account. Therefore disparities between computed and observed quantities could be large.

Geometry optimizations were performed by means of the Fletcher-Reeves conjugate gradient method.

### 3.1. Semi-empirical ZINDO/1 Modelling Scheme

ZINDO/1 is a semi-empirical method based on a modified version of the intermediate neglect of differential overlap

**Table 2**. Bond lengths (Å) and angles (degrees) for $S_2$ and $S_3$ species.

| Structure name | Symmetry | Structural parameter [a] | This work | Average from literature [b] | References |
|---|---|---|---|---|---|
| $S_2$ | $D_{\infty h}$ | r | 1.88 | 1.91 (2) | [48,49,51] |
| $S_2^-$ | $D_{\infty h}$ | r | 2.01 | 2.12 (8) | [48,57] |
| $S_2^{2-}$ | $D_{\infty h}$ | r | 2.21 (2.80) | | |
| Singlet open $S_3$ | $C_{2v}$ | $r_1$ | 1.90 | 1.98 (2) | [47,49–56] |
| | | $\alpha_1$ | 117 | 116.6 (7) | [47,49–56] |
| Singlet closed $S_3$ | $D_{3h}$ | $r_2$ | 2.08 | 2.12 (2) | [47,49–56] |
| Triplet open $S_3$ | $C_{2v}$ | $r_1$ | 1.99 | 2.00 (4) | [49,52] |
| | | $\alpha_1$ | 93 | 93 (2) | [49,52] |
| Open $S_3^-$ | $C_{2v}$ | $r_1$ | 2.00 | 2.02 (3) | [47,56,57] |
| | | $\alpha_1$ | 115 | 113 (2) | [47,56,57] |
| Closed $S_3^-$ | $D_{3h}$ | $r_2$ | 2.24 | 2.241 (5) | [47,56] |
| Open $S_3^{2-}$ | $C_{2v}$ | $r_1$ | 2.13 | 2.08 (8) | [47,57] |
| | | $\alpha_1$ | 113 | 109 (6) | [47,57] |
| Closed $S_3^{2-}$ | $D_{3h}$ | $r_2$ | 2.24 | 2.244 | [47] |

[a] As defined in Fig. 1.
[b] The value given is the average from several literature values; the number in brackets denotes one standard deviation of the mean.

(INDO) method.[42] The overlap weighting factors were set to 1 for both σ–σ and π–π interactions, as required for geometry optimization.[42]

Semi-empirical and *ab initio* methods took into account both molecular geometry and the electron distribution and the results from HyperChem[41] were interpreted in terms of the linear combination of atomic orbitals (LCAO)-molecular orbital (MO) theory.[42] These molecular orbitals were assumed to describe the motion of the electrons in molecules and the shapes of molecular orbitals to determine the reactivity of bonds in the molecule.[42]

HyperChem calculated the potential energy as a basis for geometry optimization and the force constants, vibrational modes, charge and spin densities, atomic charges, dipole moments and electrostatic charges. The electronic spectrum could also be calculated when configuration interaction was taken into account.[42] Because quantum mechanical computations deal explicitly with the electrons, it was necessary to specify the charges and spin multiplicities of the molecules.[42] When a singlet state was considered the computation was usually done with restricted Hartree-Fock (RHF) wavefunctions.[42] For higher multiplicity computations unrestricted Hartree-Fock (UHF) wave functions which distinguish between spin states were used.[42] Alpha electrons would then be in the highest occupied molecular orbital, because they were assigned first. The remainder of the electrons were assigned to beta spins.[42] The excess of alpha over beta electrons was calculated based on the number of electrons in the neutral atoms and the number of electrons lost or gained due to the charge, and on the specified multiplicity.[42]

Self-consistency was sometimes difficult to obtain, especially when degenerate states were involved.[42] To avoid this problem, HyperChem was run with a convergence accelerator, the direct inversion in the iterative subspace (DIIS) method, although the computational effort was thereby increased,[42] because the analysis of the molecular orbitals was a linear combination of the current result and the results of previous iterations.

Individual molecular orbitals could be represented on a grid in space. This was the key to deductions made regarding the reactivity of molecules, the so-called frontier orbital approach of Woodward and Hoffmann.[23–27]

The vibrational analysis and infrared spectroscopic data were obtained from the numerical Hessian matrix of second derivatives of the total energy with respect to the nuclear positions, and a normal coordinate analysis, based on mass-weighted coordinates.[42] The analysis was based on data obtained from quantum mechanical computations, but it remained classical.[42] The calculation of vibrational frequencies was described by Matsuura and Yoshida.[43]

### 3.2. *Ab Initio* Modelling Scheme

The Møller-Plesset second-order perturbation (MP2) correlation energy[44] compensated for some of the assumptions made during the Hartree-Fock computations and was used to correct the calculated energy.[42] The MP2 energy correction was done only at the energy minimum in a single point computation. This differed from its application in more advanced software packages. The *ab initio* computations in HyperChem expanded the molecular orbitals into a linear combination of atomic orbitals, without any further approximation. Several different basis sets to describe the atomic orbitals exist.[42] The 6-311G** notation implies a triple valence basis set with polarization functions.[42] The computations were performed at the self-consistent-field Hartree-Fock level of theory extended by MP2 energy correction.

*Ab initio*-determined vibrational frequencies are usually larger than observed frequencies, and need scaling.[43,45] The scale factor depended on the basis set and the level of theory used. The recommended scale factor for HF/6-311G** was 0.9051.[45] This scale factor was based on 1 066 experimental wavenumbers from 122 molecules. The molecules consisted mainly of carbon and hydrogen atoms. Krossing and Passmore,[46] however, suggested that scale factors larger than 1 be used when considering sulphur clusters. Brabson and co-workers[35] suggested a scale factor of 0.87, based on experimental data for $S_3$ and a self-consistent-field method. This scale factor was used in this work.

HyperChem supported configuration interaction (CI) only in the restricted Hartree-Fock mode. The configuration interaction computations led to the energies of the ground state and singly excited states, which were then used to calculate the electronic spectrum.[42] HyperChem could, therefore, only compute an electronic spectrum for molecules with a singlet spin state.[42] Configuration interaction was performed in one of two ways, either as a singly excited state or as a microstate. The electrons were allowed to exchange from a limited number of occupied to a limited number of unoccupied orbitals. Configuration interaction was used to obtain a more accurate set of states by taking appropriate linear combinations of these microstates or singly excited states.[42]

**Table 3**. Relative energies of $S_2$ species [a].

| Structure number | Structure name | Relative energy/kJ mol$^{-1}$ |
|---|---|---|
| 2 | $S_2$ singlet | 146 |
| 2 | $S_2$ triplet | 113 |
| 2 | $S_2^-$ | 0 |
| 2 | $S_2^{2-}$ singlet | 427 |
| 2 | $S_2^{2-}$ triplet | 632 [b] |

[a] Energies are reported relative to the most stable isomer, taken as zero.
[b] Species has an imaginary frequency.

## 4. Results

Compared with literature values the geometry optimization gave reasonable results (Table 2). As the charge on the $S_2$ species became more negative the bond distance increased (Table 2). The geometry of the closed, $D_{3h}$, $S_3^{-\bullet}$ isomer did not optimize to the desired symmetry and the bond length was therefore set to the average of the values found in the literature (Table 2). The geometry of the closed $S_3^{2-}$ isomer optimized to unrealistically long bond lengths, and the bond distance was set to 2.24 Å.[47] The singly negative anions of both $S_2$ and $S_3$ were found to be the most stable states relative to the neutral and doubly charged states (Tables 3 and 4). Our results at the UHF/6-311G** level of theory indicated that the open, $C_{2v}$, structure was the most stable isomer for the $S_3^{-\bullet}$ molecule (Table 4). In fact, at this level, the closed, $D_{3h}$, $S_3^{-\bullet}$ geometry was shown to be a transition state.

The calculated vibrational wavenumbers for $S_2$, $S_2^{-\bullet}$ and $S_2^{2-}$ were in good agreement with the experimental values (Table 5). For $S_2^{2-}$ the unscaled wavenumbers fit best (Table 5). The vibrational wavenumber decreased with an increase in the negative charge on the $S_2$ molecule as expected from the reverse trend in the bond distances (Table 2). After applying the scale factor of 0.87 to the calculated wavenumbers (Table 6) of the open $S_3$ isomer, they corresponded well with experimental values (Tables 1 and 6). The scaled vibrational wavenumbers of the closed, $D_{3h}$, $S_3$ isomer (Table 7) agreed with the experimental values. The calculated vibrational wavenumbers of $S_3^{-\bullet}$ were less accurate (Table 8). The antisymmetric stretching wavenumber was underestimated, even before scaling. For $S_3^{2-}$, the vibrational wavenumbers were close to the experimental values without scaling (Table 8).

Molecular modelling of the polysulphide species was done in order to obtain a molecular orbital picture of $S_2^{-\bullet}$ (Fig. 3), and $S^{+\bullet}$ and $S_3^{-\bullet}$ (Fig. 4). HyperChem[41] was used to model the $S_2^{-\bullet}$ and $S_3^{-\bullet}$ structures by the ZINDO/1 semi-empirical method, and self-consistent-field unrestricted Hartree-Fock simulation using a 6-311G** basis set extended by MP2 correlation energy. The ZINDO/1 results confirmed the character of the highest occupied molecular orbital for both open ($b_1$) and closed ($a_2'$) $S_3^{-\bullet}$ of a

**Table 4**. Relative energies of $S_3$ species [a].

| Structure number | Structure name | Relative energy/kJ mol$^{-1}$ |
|---|---|---|
| 3 | Open $S_3$ singlet | 197 |
| 4 | Closed $S_3$ singlet | 234 |
| 3 | Open $S_3$ triplet | 297 |
| 4 | Closed $S_3$ triplet | 473 [b] |
| 3 | Open $S_3^-$ | 0 |
| 4 | Closed $S_3^-$ | 192 [b] |
| 4 | Closed $S_3^{2-}$ singlet | 720 [b] |
| 3 | Open $S_3^{2-}$ singlet | 331 |
| 4 | Closed $S_3^{2-}$ triplet | 682 [b] |
| 3 | Open $S_3^{2-}$ triplet | 577 [b] |

[a] Energies are reported relative to the most stable isomer, taken as zero.
[b] Species has an imaginary frequency.

**Table 5**. Vibrational wavenumbers (cm$^{-1}$) of $S_2$ stretching vibration.

| Species | This work | Scaled values | Experimental | References |
|---|---|---|---|---|
| Singlet $S_2$ | 791 | 687 | 724 | [32] |
| Triplet $S_2$ | 790 | 687 | | |
| Doublet $S_2^{-\bullet}$ | 615 | 535 | 590 | [2,5] |
| Singlet $S_2^{2-}$ | 426 | 371 | 451 | [33] |

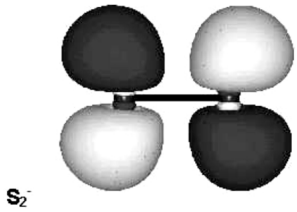


**Figure 3**. Highest occupied and lowest unoccupied molecular orbitals of $S_2^{-\bullet}$

**Table 6**. Vibrational wavenumbers (cm$^{-1}$) of open $S_3$ (**1**).

| Mode | Description | Symmetry | This work | Scaled values [a] | Experimental values [b] | Spectroscopic activity [c] |
|---|---|---|---|---|---|---|
| $\nu_1$ | Symmetric stretching | $a_1$ | 654 (627) | 569 | 575 | R, IR |
| $\nu_2$ | Bending | $a_1$ | 294 (211) [d] | 256 | 256 | R, IR |
| $\nu_3$ | Antisymmetric stretching | $b_2$ | 737 (490) | 641 | 656 | R, IR |

[a] Scaled with a scale factor of 0.87 (see ref. 35).
[b] Reference 36.
[c] R: Raman active; IR: infrared active.
[d] Values in brackets are for the triplet state.

**Table 7**. Vibrational wavenumbers (cm$^{-1}$) of closed $S_3$ (**2**).

| Mode | Description | Symmetry | This work | Scaled values [a] | Experimental values | Spectroscopic activity [b] |
|---|---|---|---|---|---|---|
| $\nu_1$ | Symmetric stretching | $a_1'$ | 662 | 576 | 583[35], 585[34], 575[36] | R |
| $\nu_2$ | Deformation | $e'$ | 500 | 435 | 450[35,39], 490[34] | R, IR |

[a] Scaled with a scale factor of 0.87 (reference 35).
[b] R: Raman active; IR: infrared active.

**Table 8**. Vibrational wavenumbers ($cm^{-1}$) of negatively charged open $S_3$ (**1**).

| Mode | Description | Symmetry | $S_3^{-\bullet}$ doublet | $S_3^{-\bullet}$ singlet | $S_3^{2-}$ open | | Spectroscopic activity [a] |
|---|---|---|---|---|---|---|---|
| | | | Calculated | Experimental | Calculated (ref. 37) | Experimental | |
| $\nu_1$ | Symmetric stretching | $a_1$ | 558 | 548[2] | 459 | 458 | R, IR |
| $\nu_2$ | Bending | $a_1$ | 250 | 232[40] | 202 | 227/238 | R, IR |
| $\nu_3$ | Antisymmetric stretching | $b_2$ | 449 | 582[2] | 496 | 476 | R, IR |

[a] R: Raman active; IR: infrared active

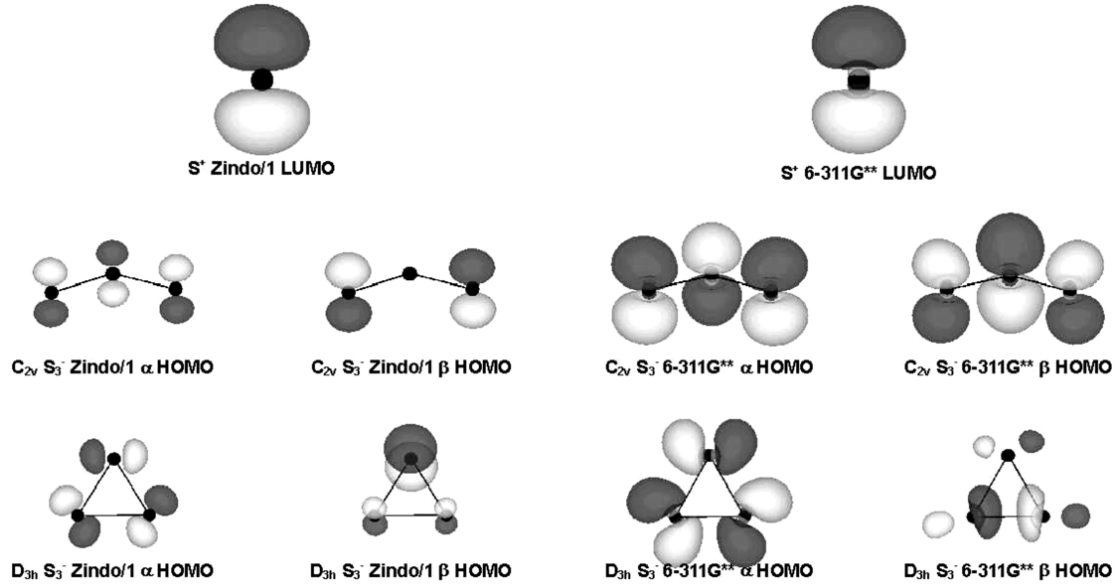


**Figure 4**. Molecular orbital diagram of $S^{+\bullet}$ (ZINDO/1 and 6-311G** LUMO) and $S_3^{-\bullet}$ (ZINDO/1 and 6-311G** α and β HOMO)

previous pictorial model[22] and the work of Koch and co-workers[47] (Fig. 4).

It was assumed that $S^{+\bullet}$ (Fig. 4) attacked the $S_3^{-\bullet}$ (Fig. 4) species in a concerted reaction to form $S_4$ (Fig. 2). The validity of different isomers as potential products was tested by means of the frontier orbital symmetry theory of Woodward and Hoffmann.[25–27] The HOMO of $S_3^{-\bullet}$ (Fig. 4) was placed near the LUMO of $S^{+\bullet}$ (Fig. 4) in such a way as to ensure that lobes of the same phase overlapped to form σ-orbitals. Other orientations of the $S^{+\bullet}$ molecular orbital were possible. The charge distribution on the sulphur atoms of the $S_3^{-\bullet}$ isomers indicated that the central sulphur atom was positively charged (Fig. 5), therefore attack of $S^{+\bullet}$ was unlikely to occur at this atom. To test whether the electrostatic charges would be unfavourable to this form of attack the distance between the fourth sulphur atom and the central sulphur atom, in the branched chain isomer, was increased (Fig. 5). The

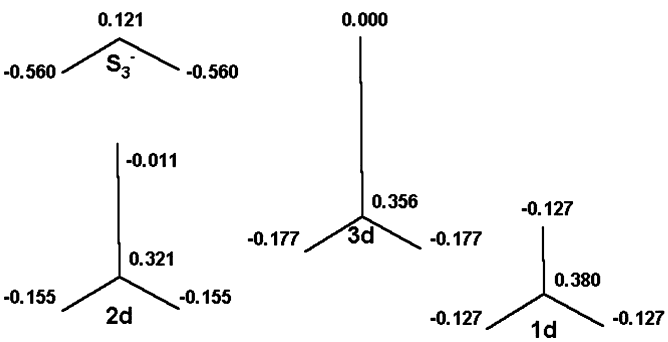


**Figure 5**. Charge distribution in $S_3^{-\bullet}$ and branched chain $S_4$ at three times (3d), twice (2d) and at its normal distance (1d).

induced charge distribution is similar to the original charge distribution in the $S^{3-\bullet}$ moiety, in that the central atom is positive relative to the terminal sulphur atoms, therefore the positive charge on the central sulphur atom in $S_3^{-\bullet}$ is not necessarily a problem in the formation of the branched chain $S_4$ from $S_3^{-\bullet}$ and $S^{+\bullet}$.

A Woodward-Hoffmann analysis at the ZINDO/1 level showed that the puckered $S_4$ ring (6), pyramidal branched chain $S_4$ (15), gauche $S_4$ chain (4), double triangle (10) and bent exocyclic $S_4$ (16) isomers were possible products of the concerted reaction of $S^{+\bullet}$ and $S_3^{-\bullet}$. Using the 6-311G** basis set, the highest occupied molecular orbital of the closed, $D_{3h}$, $S_3^{-\bullet}$ isomer precluded the formation of the bent exocyclic $S_4$ (16) isomer.

Furthermore, the symmetry of the highest occupied and lowest unoccupied molecular orbitals of $S_2^{-\bullet}$ (Fig. 3) predicted that the closed, $D_{3h}$, $S_3^{-\bullet}$ isomer could not be formed from $S_2^{-\bullet}$ in a concerted way.

## 5. Discussion

Computational results should not be accepted at face value because of the approximations made during the analysis. Strictly speaking, *ab initio* computations are only relevant to gas phase molecules in vacuum at 0 K. The environment created by the sodium counterions and the aluminosilicate framework was not taken into account. The structure of the aluminosilicate framework did ensure that the sulphur chromophores acted independently as molecules and did not form part of an extended sulphur-based 'molecule'.

The calculated wavenumber of $S_2$ at 793 $cm^{-1}$, scaled (0.87) to 690 $cm^{-1}$, was in reasonable agreement with the experimental value of 724 $cm^{-1}$ (Table 5). The bond length of 1.88 Å was in close

agreement with the experimental 1.893 Å.[30,31] Heinemann and co-workers[48] calculated the vibrational wavenumber of $S_2^{-\bullet}$ to be 582 $cm^{-1}$, close to the experimental value (Table 5). The current value was not far from the expected value (Table 5). Heinemann and co-workers[48] calculated that the triplet $S_2$ molecule was less energetic than the $S_2^{-\bullet}$ molecule. The current results confirm this.

Rau and co-workers[58] suggested that sulphur allotrope tautomers with an energy difference less than 33 kJ $mol^{-1}$ contributed appreciably to the vapour composition of that particular species at temperatures between 823 and 1273 K. This was suggested on the basis of the work of Pauling,[59] who mentioned the estimate of tautomeric occurrence at 41 kJ $mol^{-1}$. Therefore, sulphur allotropic isomers found, in this work, to have an energy difference of less than 41 kJ $mol^{-1}$ relative to the most stable isomer should be present in appreciable amounts.

The bond angle calculated for the open $S_3$ isomer was 117°, which is within the experimental range.[35] The question of whether the open, $C_{2v}$,[47,49,52,53,55,56] or closed, $D_{3h}$,[48,55,56,60,61] $S_3$ isomer was the more stable seemed to be an open question, since several methods gave contradictory results, depending on the methodology applied to the problem. The open, $C_{2v}$, $S_3$ isomer was calculated to be the more stable in this work. The computed closed, $D_{3h}$, $S_3$ isomer had an energy only 37 kJ $mol^{-1}$ higher than that of the open isomer, therefore both these isomers should be observable (Table 4) and probably were (Tables 6 and 7).

From the literature it seemed as though the open, $C_{2v}$,[47,54] $S_3^{-\bullet}$ isomer was deemed to be more stable than the closed, $D_{3h}$, isomer. This was confirmed in the current work. The scale factor of 0.87, suggested by Brabson and co-workers,[35] worked well for the neutral sulphur molecules (Tables 5–7), but failed for the ionized species (Tables 5 and 8). Since the $S_3^{-\bullet}$ molecule is the blue chromophore in ultramarine blue,[1,2,5,8,9] the geometry of this important stable radical polysulphide was calculated, and found to be $C_{2v}$. This geometry could now be used in modelling the ultramarine pigment itself,[62] and could assist in crystallographic interpretation.[17]

The reaction that transforms ultramarine green to blue is exothermic.[12] The calculated results (Tables 3 and 4) supported the proposal that this reaction involves the transition from $S_2^{2-}$, $S_3^{2-}$ to $S_2^{-\bullet}$, $S_3^{-\bullet}$.[1,11–15]

The assumption that the $S_4$ molecules were formed by concerted reactions of $S_3^{-\bullet}$ and $S^{+\bullet}$ was theoretically useful, although the existence of $S^{+\bullet}$ was unlikely, even though it had been observed in photoionization experiments.[63]

Based on the fact that the tetrahedral geometry of $S_4$ has an open-shell electronic configuration, Salahub and co-workers[54] ruled out the tetrahedral geometry as the ground state of $S_4$ by Xα-scattered wave calculations. This conclusion was also reached by Landman and De Waal based on Woodward-Hoffmann selection rules,[22] and was verified in the current work. The puckered $S_4$ ring (6), and especially the double triangle $S_4$ (10) would probably not be the most stable isomers due to internal ring strain. The pyramidal branched chain $S_4$ isomer (15) also seemed unlikely to be the most stable isomer, based on the close proximity of the sulphur atoms. The gauche $S_4$ chain (4) was likely to be the energy minimum for the $S_4$ isomers, due to the strain and interaction-free geometry.

## 6. Conclusion

At the UHF/6-311G** level of theory the open, $C_{2v}$, structure was found to be the more stable isomer for the $S_3^{-\bullet}$ molecule, which was the blue chromophore in ultramarine. The closed, $D_{3h}$, geometry was calculated to be a transition state (Table 4). For both $S_2$ and $S_3$ the singly negative anion was calculated to be the most stable state, in relation to the neutral and doubly-charged states (Tables 3 and 4), and supported the proposal that this reaction involved the transition from $S_2^{2-}$, $S_3^{2-}$ to $S_2^{-\bullet}$, $S_3^{-\bullet}$.[1,11–15]

Woodward-Hoffmann orbital analyses and steric interactions indicated that the gauche chain $S_4$ (4) was the most probable $S_4$ isomer in ultramarine red.

## Acknowledgements

This work was supported by a grant from the Technology and Human Resources for Industry Programme (THRIP), a partnership programme funded by the Department of Trade and Industry (DTI) and managed by the National Research Foundation (NRF). The financial assistance of the Department of Labour (DoL) towards this research is hereby acknowledged. Opinions expressed and conclusions arrived at, are those of the authors and are not necessarily to be attributed to the DoL. The authors also wish to thank Sphere-Fill (Pty) Ltd and the University of Pretoria for financial support. Professor Jan C.A. Boeyens is thanked for useful discussions and recommendations.

## References

1 W.B. Cork, *Ultramarine Pigments*, in *Industrial Inorganic Pigments*, G. Buxbaum (ed.), VCH, Weinheim, Germany, 1993, pp. 124–132.
2 R.J.H. Clark and D.G. Cobbold, *Inorg. Chem.*, 1978, **17**, 3169–3174.
3 H. He, T.L. Barr and J. Klinowski, *J. Phys. Chem.*, 1994, **98**, 8124–8127.
4 K-H. Schwarz and U. Hofmann, *Z. Anorg. Allgem. Chem.*, 1970, **378**, 152–159.
5 R.J.H. Clark, T.J. Dines and M. Kurmoo, *Inorg. Chem.*, 1983, **22**, 2766–2772.
6 U. Hofmann, E. Herzenstiel, E. Schonemann and K-H. Schwarz, *Z. Anorg. Allgem. Chem.*, 1969, **367**, 119–129.
7 J. Klinowski, S.W. Carr, S.E. Tarling and P. Barnes, *Nature*, 1987, **330**, 56–58.
8 N. Gobeltz, A. Demortier, J. P. Lelieur and C. Duhayon, *J. Chem. Soc., Faraday Trans.*, 1998, **94**, 2257–2260.
9 D.M. Gruen, R.L. McBeth and A.J. Zielen, *J. Am. Chem. Soc.*, 1971, **93**, 6691–6693.
10 P. Köhler, G. Winter, F. Seel and K-P. Klös, *Z. Naturforsch.*, 1987, **42b**, 663–665.
11 A. E. Gorshtein, *J. Appl. Chem. USSR*, 1985, **58**, 1468–1473.
12 A.P. Beardsley and S.H. Whiting, Manufacture of Ultramarine, Final Patent no. 2 441 952, United States, 25 May 1948.
13 A.P. Beardsley and S.H. Whiting, Production of Ultramarine, Final Patent no. 2 441 951, United States, 25 May 1948.
14 A.E. Gorshtein, *Can. J. Chem. Eng.*, 1992, **70**, 960–965.
15 A.P. Beardsley and S.H. Whiting, Manufacture of Ultramarine, Final Patent no. 2 441 950, United States, 25 May 1948.
16 A.A. Landman and D. de Waal, *Materials Res. Bull.*, 2004, **39**, 655–667.
17 S.E. Tarling, P. Barnes and A.L. Mackay, *J. Appl. Cryst.*, 1984, **17**, 96–99.
18 T. Chivers and I. Drummond, *Chem. Soc. Rev.*, 1973, **2**, 233–248.
19 M.T. Weller, G. Wong, C.L. Adamson, S.M. Dodd and J.J.B. Roe, *J. Chem. Soc., Dalton Trans.*, 1990, 593–597.
20 N. Gobeltz-Hautecoeur, A. Domortier, B. Lede, J.P. Lelieur and C. Duhayon, *Inorg. Chem.*, 2002, **41**, 2848–2854.
21 F. Seel, H-J. Güttler, A. B. Wiecowski and B. Wolf, *Z. Naturforsch.*, 1979, **34b**, 1671–1677.
22 A.A. Landman and D. De Waal, *Cryst. Eng.*, 2001, **4**, 159–169.
23 K. Fukui, *Tetrahedron Letters*, 1965, **28**, 2427–2432.
24 K. Fukui, *Tetrahedron Letters*, 1965, **24**, 2009–2015.
25 R.B. Woodward and R. Hoffmann, *J. Am. Chem. Soc.*, 1965, **87**, 2046–2048.
26 R.B. Woodward and R. Hoffmann, *J. Am. Chem. Soc.*, 1965, **87**, 2511–2513.
27 R.B. Woodward and R. Hoffmann, *J. Am. Chem. Soc.*, 1965, **87**, 395–397.
28 F.A. Carey and R.J. Sundberg, *Advanced Organic Chemistry, Part A:*

*Structure and Mechanisms,* 3rd edn., Plenum Press, New York, 1990, pp. 595–640.

29 M. Sannigrahi and F. Grein, *Can. J. Chem.*, 1994, **72**, 298–303.

30 S.M. Naudé, *Nature*, 1945, **155**, 426–427.

31 S.M. Naudé, *S. Afr. J. Science*, 1945, **41**, 128–151.

32 R. Maeder and E. Miescher, *Nature*, 1948, **161**, 393.

33 G.J. Janz, J.R. Downey, E. Roduner, G.J. Wasilczyk, J.W. Coutts and A. Eluard, *Inorg. Chem.*, 1976, **15**, 1759–1763.

34 A.G. Hopkins, S-Y. Tang and C.W. Brown, *J. Am. Chem. Soc.*, 1973, **95**, 3486–3494.

35 G.D. Brabson, Z. Mielke and L. Andrews, *J. Phys. Chem.*, 1991, **95**, 79–86.

36 P. Lenain, E. Picquenard, J.L. Lesne and J. Corset, *J. Mol. Struct.*, 1986, **142**, 355–358.

37 G.J. Janz, E. Roduner, J.W. Coutts and J.R. Downey, *Inorg. Chem.*, 1976, **15**, 1751–1754.

38 G.J. Janz, J.W. Coutts, J.R. Downey and E. Roduner, *Inorg. Chem.*, 1976, **15**, 1755–1759.

39 P. Hassanzadeh and L. Andrews, *J. Phys. Chem.*, 1992, **96**, 6579–6585.

40 T. Chivers and I. Drummond, *Inorg. Chem.*, 1972, **11**, 2525–2527.

41 HyperChem, ver. 6.03 for Windows, distributed by HyperCube Inc., Gainesville, Florida, U.S.A., 2000.

42 HyperChem Computational Chemistry, HyperCube Inc., Waterloo, Canada, 1996.

43 H. Matsuura and H. Yoshida, Calculation of vibrational frequencies by hartree-fock-based and density functional theory, in *Handbook of Vibrational Spectroscopy*, J. M. Chalmers and P. R. Griffiths (ed.), vol. 3, John Wiley & Sons, New York, 2002, pp. 2012–2028.

44 C. Møller and M.S. Plesset, *Phys. Rev.*, 1934, **46**, 618–622.

45 A.P. Scott and L. Radom, *J. Phys. Chem.*, 1996, **100**, 16502–16513.

46 I. Krossing and J. Passmore, *Inorg. Chem.*, 1999, **38**, 5203–5211.

47 W. Koch, J. Natterer and C. Heinemann, *J. Chem. Phys.*, 1995, **102**, 6159–6167.

48 C. Heinemann, W. Koch, G-G. Lindner and D. Reinen, *Phys. Rev. A*, 1995, **52**, 1024–1038.

49 D. Hohl, R.O. Jones, R. Car and M. Parinello, *J. Chem. Phys.*, 1988, **89**, 6823–6835.

50 W.G. Laidlaw and M. Trsic, *Chem. Phys.*, 1979, **36**, 323–325.

51 B. Meyer and K. Spitzer, *J. Phys. Chem.*, 1972, **76**, 2274–2279.

52 K. Raghavachari, C. M. Rohlfing and J. S. Binkley, *J. Chem. Phys.*, 1990, **93**, 5862–5873.

53 M. Morin, A.E. Foti and D.R. Salahub, *Can. J. Chem.*, 1985, **63**, 1982–1987.

54 D.R. Salahub, A.E. Foti and V. H. Smith, *J. Am. Chem. Soc.*, 1978, **100**, 7847–7858.

55 J.E. Rice, R. D. Amos, N.C. Handy, T.J. Lee and H.F. Schaefer, *J. Chem. Phys.*, 1986, **85**, 963–968.

56 V.G. Zakrzewski and W. von Niessen, *Theoret. Chim. Acta*, 1994, **88**, 75–96.

57 F.A. Cotton, J. B. Harmon and R.M. Hedges, *J. Am. Chem. Soc.*, 1976, **98**, 1417–1424.

58 H. Rau, T.R.N. Kutty and J.R.F. Guedes de Carvalho, *J. Chem. Thermodyn.*, 1973, **5**, 833–844.

59 L. Pauling, *Proc. Nat. Acad. Sci. USA*, 1949, **35**, 495–499.

60 K. Jug and R. Iffert, *J. Mol. Struct. (Theochem)* , 1989, **186**, 347–359.

61 W. von Niessen and P. Tomasello, *J. Chem. Phys.*, 1987, **87**, 5333–5337.

62 M.C. Gordillo and C.P. Herrero, *J. Phys. Chem.*, 1993, **97**, 8310–8315.

63 J. Berkowitz and W.A. Chupka, *J. Chem. Phys.*, 1969, **50**, 4245–4250.